

Full Length Research Paper

The impact of wind power plant with doubly fed induction generator on the power systems

Trinh Trong Chuong

Department of Power Systems, Faculty of Electrical Engineering, Hanoi University of Industry, Vietnam.
5th Floor, A10 Building, Block A, Hanoi University of Industry; km 13, MinhKhai Village, TuLiem District, Hanoi, Vietnam.
E-mail: chuonghtd@gmail.com. Tel: (+84)0904 993 611.

Accepted 10 July, 2011

Recently, Wind Power Plant (WPP) has been experiencing a rapid development in a global scale. The size of wind turbines and wind power plants are increasing quickly; a large amount of wind power is integrated into the power system. As the wind power penetration into the grid increases quickly, the influence of wind turbines on the dynamic stability is becoming more and more important. This paper studies the effect of wind power plants with double fed induction generator (DFIG) on the electric power system operation. The important characteristics such as: Voltage quality, grid voltage stability, active and reactive loss of a DFIG at different fault conditions studied. The simulation results clearly show the effect of wind power plants on the grid voltage stability and power quality of electric power system.

Key words: Wind power, double fed induction generator (DFIG), voltage stability, power - voltage curve (PV).

INTRODUCTION

As a result of conventional energy sources consumption and increasing environmental concern, efforts have been made to generate electricity from renewable sources, such as wind energy sources. Institutional support on wind energy sources, together with the wind energy potential and improvement of wind energy conversion technology, has led to a fast development of wind power generation in recent years. Other reasons could be the fuel price but especially environmental demands. The wind generation does not pollute the surrounding areas and also does not produce waste products (Sujatha, 2006). To get the maximum possible power, the wind generator speed should change according to the wind speed.

Generally the wind turbines (WT) can either operate at fixed speed or variable speed. For a fixed speed WT, the generator is directly connected to the electrical grid. The rotor speed of the fixed speed WTs is in principle determined by a gearbox and the pole-pair number of the generator. An impediment of the fixed speed WT is that power quality of the output power is poor. For a variable speed WT equipped with a converter connected to the stator of the generator, the generator could either be a cage bar induction generator, synchronous generator or permanent-magnet synchronous generator. There are several reasons for using variable speed operation of

WTs; among those are possibilities to reduce stresses of the mechanical structure, acoustic noise reduction and the possibility to control active and reactive power (Francoise and Bikash, 2005). An important type of variable speed WT is WT with double fed induction generator (DFIG). This means that the stator is directly connected to the grid while the rotor winding is connected via slip rings to a back-to-back converter (Figure 1). Today, DFIG are commonly used by the WT industries for larger WTs (Joris, 2005).

The major advantage of the DFIG, which has made it popular, is that the power electronic equipment only has to handle a fraction (20 to 30%) of the total system power (Johannes, 2003). This means that the cost of the power electronic equipment and the losses in the equipment can be reduced in comparison to power electronic equipment that has to handle the total system power as for a direct-driven synchronous generator, apart from the cost saving of using a smaller converter (James, 1988).

WIND TURBINE WITH DFIG

For variable speed systems with limited variable-speed range ($\pm 30\%$ of synchronous speed), the DFIG can be a cost effective solution. The DFIG converter consists of

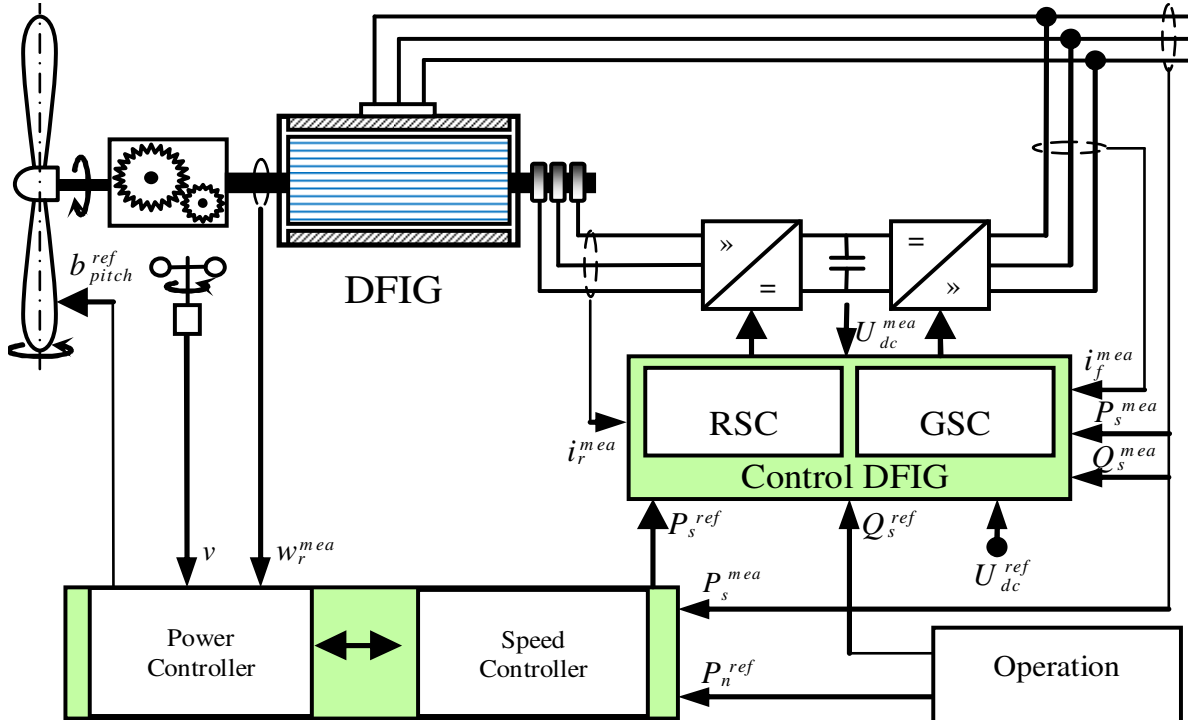


Figure 1. General structure of the DFIG.

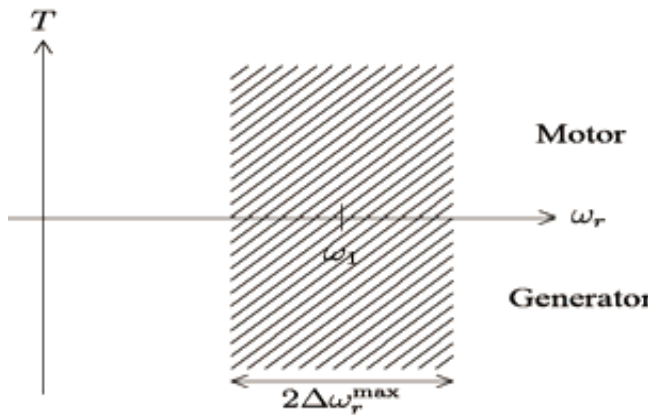


Figure 2. Speed torque characteristics of a DFIG.

two converters that are connected “back-to-back” as in Figure 1; machine-side converter and grid side converter. Between the converter, a dc-link capacitor is placed, as energy storage to keep the dc-link voltage variations (or ripple) small.

With the machine side converter, it is possible to control the torque or the speed of the DFIG, and also the power factor at the stator terminals, while the main objective for the grid-side converter is to keep the dc-link voltage constant. The speed torque characteristics of the DFIG system can be seen in Figure 2 (Johannes, 2003; Tony et al., 2004). As also seen in the figure, the DFIG

can operate both in motor and generator operation with a rotor-speed range of $\pm\Delta\omega_r$ max around the synchronous speed.

WT-DFIG model description

The complete model of a WT-DFIG is constructed from a number of sub models, that is, (a) turbine, (b) drive train, (c) pitch controller, (d) wound-rotor induction generator, (e) rotor-side converters. The general structure of the model is shown in Figure 1.

Turbine model

One common way to control the active power of a WT is by regulating the C_p value of the rotor turbine. In the model, the C_p value of the turbine rotor is approximated using a non-linear function according to Joris (2005) and Tony et al. (2004).

$$P_m = \frac{1}{2} \rho A_T C_p (\lambda, \beta) \cdot v_{wind}^3;$$

$$C_p (\lambda, \beta) = 0.22 \left(\frac{116}{\lambda_i} - 0.4 \beta - 5 \right) e^{-\frac{12.5}{\lambda_i}}$$

$$\frac{1}{\lambda_i} = \frac{1}{\lambda + 0.008 \beta} - \frac{0.035}{\beta^3 + 1}$$

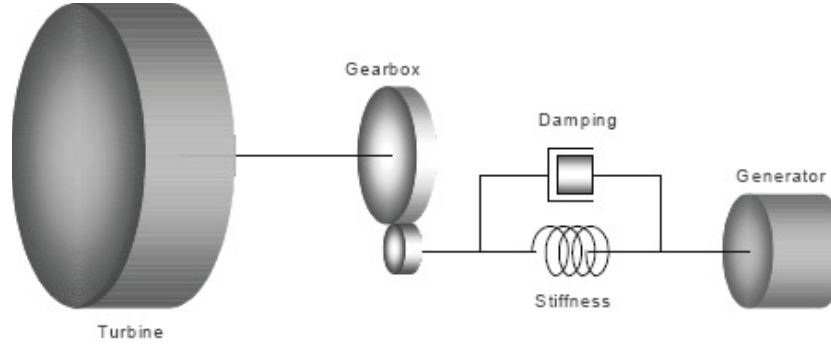


Figure 3. Drive- train system of WT-DFIG.

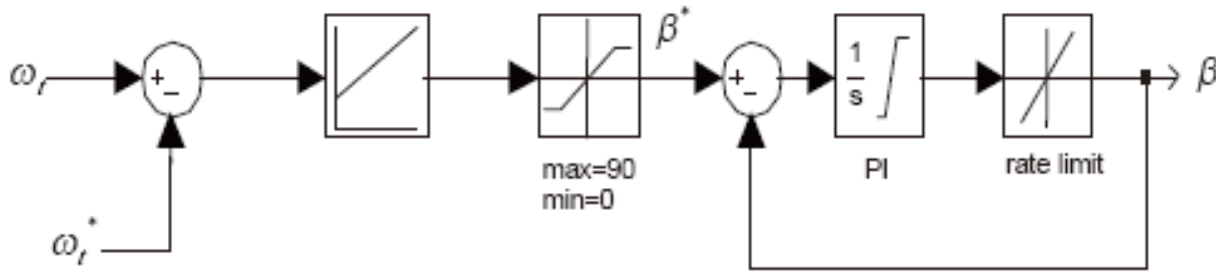


Figure 4. Pitch controller diagram.

where C_p is the power coefficient, β is the pitch angle, λ is the tip speed ratio, ω_{wind} is the wind speed, ω_r is the rotor speed, r is the rotor-plane radius, ρ is the air density and A_r is the area swept by the rotor.

Drive-train model

When investigating dynamic stability, it is important to include the drive-train system of a WT in the model. Its model consists of two main masses; the turbine mass and generator mass (Figure 3). These are connected to each other via a shaft that has certain stiffness and damping constant values. The equation of the turbine side is given as:

$$\begin{aligned}
 2H_t \frac{d\omega_t}{dt} &= T_t - K_s \cdot \theta_{tg} - D_s \cdot (\omega_t - \omega_g) \\
 2H_g \frac{d\omega_g}{dt} &= T_g + K_s \cdot \theta + D_s \cdot (\omega_t - \omega_g) \\
 \frac{d\theta_{tg}}{dt} &= \omega_{base} (\omega_t - \omega_g)
 \end{aligned} \tag{2}$$

Where H is the inertia constant, T is torque and ω is angular speed. Subscripts g and t indicate the generator and turbine quantities, respectively. The shaft stiffness

and damping constant value are represented in K_s and D_s , ω_{base} is the base value of angular speed.

Pitch controller model

According to Equation (2), the C_p (power coefficient) value can be reduced by increasing the pitch angle β . However, the pitch angle is not able to reach the set point value immediately. Accordingly, for a more realistic simulation, a rate limiter is implemented in the pitch controller model.

The pitch angle controller block diagram, shown in Figure 4, is employed to limit the rotor speed. For this reason, the pitch-angle controller is active only during high average wind speed (Johannes, 2003).

Generator model

The generator is basically a slip-ring induction machine, which can be modeled according to Francoise and Bikash (2005) by the following equation:

$$\begin{aligned}
 u_s &= R_s \cdot i_s + \frac{d}{dt}(\psi_s) + (\omega_a - \omega_s) \psi_s \\
 u_r &= R_r \cdot i_r + \frac{d}{dt}(\psi_r) + (\omega_a - \omega_r) \psi_r
 \end{aligned} \tag{3}$$

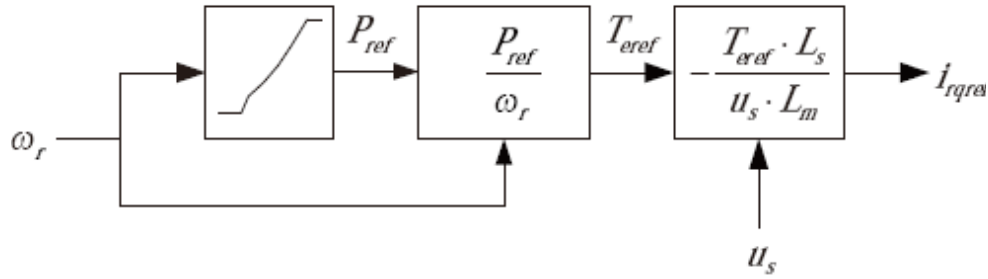


Figure 5. Active power control diagram.

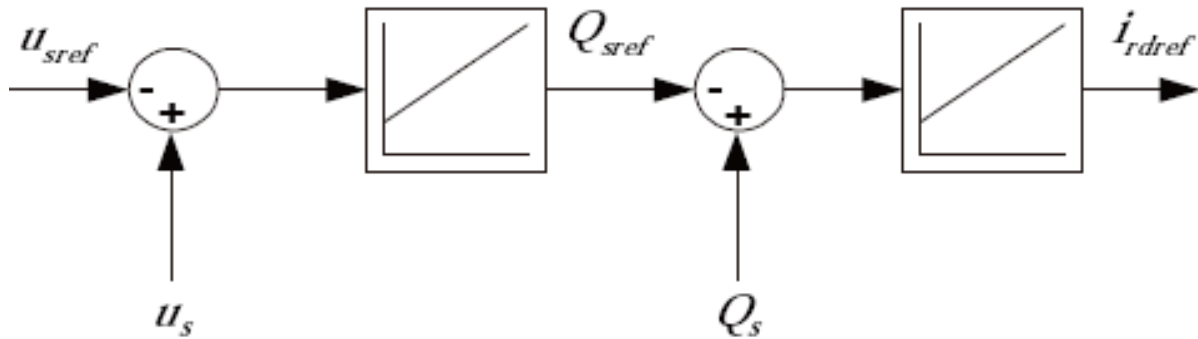


Figure 6. Reactive power and voltage control diagram.

Where u , i , and ψ are vectors of voltage, current, and flux those are functions of time, and R is the resistance. Subscripts s and r denote the stator and rotor quantities. The speed of the rotor is denoted by ω_r . The equations are given in an arbitrary reference frame, which rotates at arbitrary speed of ω_a . The flux and current relations are given as:

$$\begin{aligned} \psi_s &= (L_{sl} + L_m)i_s + L_m.i_r \\ \psi_r &= (L_{rl} + L_m)i_r + L_m.i_s \end{aligned} \quad (4)$$

Where L_m is the mutual inductance and L_{sl} and L_{rl} are the stator and rotor leakage inductances, respectively.

The rotor side converters controller model

The rotor side converter is modeled as a voltage source type. For simplification, switching phenomena and dynamic limitations in the converter are neglected by assuming that switching frequency is infinite. The purpose of the controller is to regulate the active and reactive power output independently. To decouple these two parameters, generator quantities are calculated using vector control in a synchronous reference frame fixed to the stator flux. The controller provides set point values of the quadrature and direct axis component of the rotor current (i_{qr} and i_{dr}) (Johannes, 2003). The active power is controlled as shown in Figure 5. A generic model of the

voltage and reactive power control is arranged in a cascaded mode as shown in Figure 6.

The DFIG can be operated to implement, either constant reactive power control, or controlled terminal voltage. In this paper, the first method is employed.

SYSTEM UNDER STUDY

The studied model represents an equivalent of the PhuocNinh, NinhThuan, Vietnam (Figure 7) system in the area where large scale wind power production is located (RISØ National Laboratory, 2006). The model represents a 20 MW wind power station consisting 10 turbines with DFIG connected to the grid. The turbines are stall regulated type, with a rating of 2.0 MW each. Figure 9 shows the equivalent model of the system. $Z_{th} = (0.00125 + j0.005)$ (Trinh, 2008). Sending end voltage is constant. In order to investigate the impact of the injection of active power by the wind power plant (WP) the system is approximated to a series of impedances as indicated in Figure 9.

SIMULATION

To investigate the impact of operating the WT DFIG on the power grid, two configurations are distinguished: (1) Grid and load alone, and (2) Grid, load and WP. The

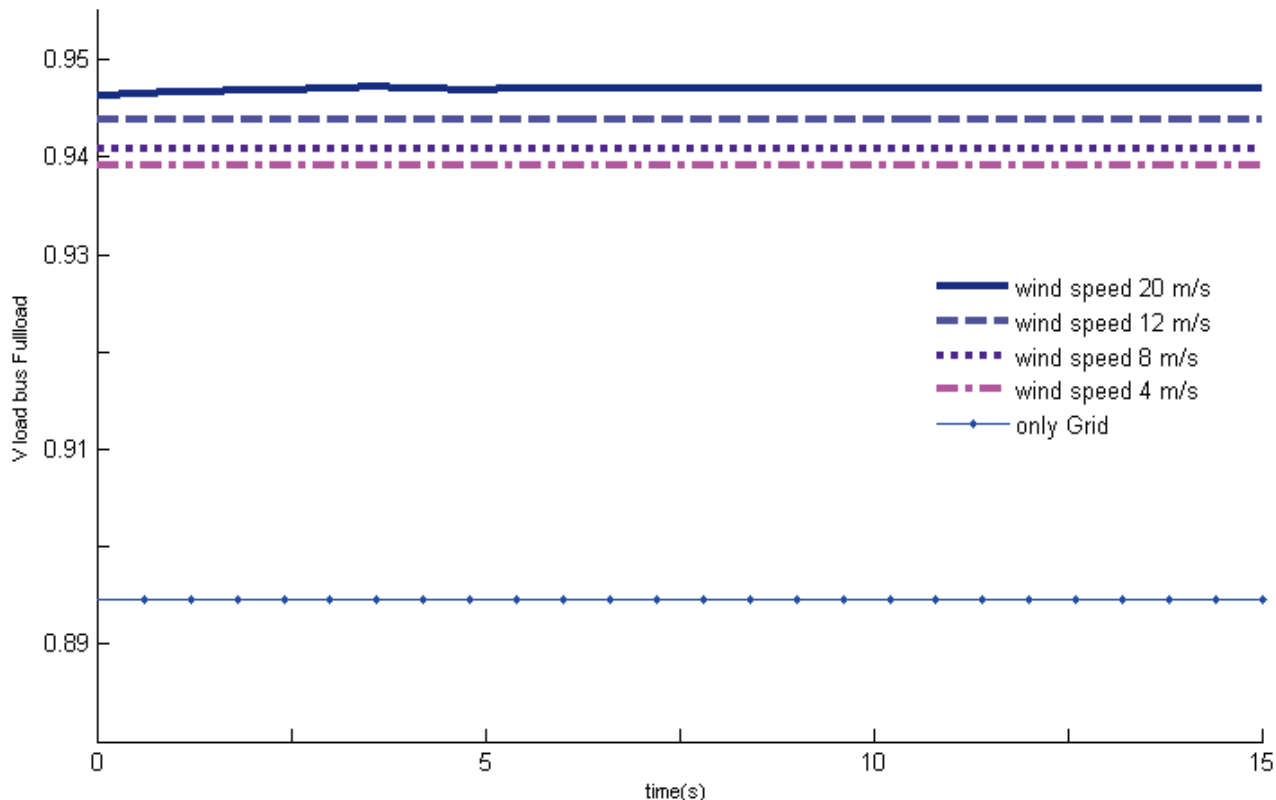


Figure 8. Steady-state voltage profile for conditions (a) and (b).

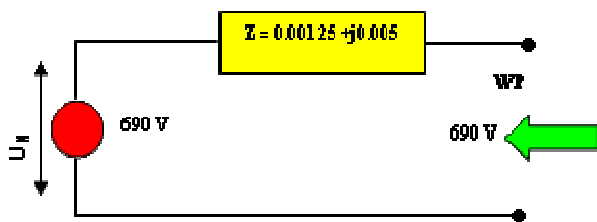


Figure 9. Equivalent grid and connection system impedance as seen from the low voltage (690 V).

into one. The transformer that is normally located at the base of each machine is, therefore, also combined into one item.

For this option, the voltage profile at the generator terminals is required and therefore all the impedances need to be reflected to the voltage level at the generator, that is, 690 V. This calculation is worked through in the sections that follow. In order to investigate the impact of the injection of active power by the WP, the system is approximated to a series of impedances as indicated in Figure 9 (Trinh, 2008).

In Figure 9, Z_{th} is the Thevenin equivalent impedance of the grid up to the Point of Common Coupling (PCC) and the connection equipment up and until the point being considered. The impedance is composed of both resistance (R_{th}) and reactance (X_{th}). In mathematical

terms, the resistance is a real number and the reactance an imaginary number, hence it is " jX_{th} ". This is the impedance that represents the WPP. The resistive (real, R_{WPF}) component is negative so that current and hence active power is produced. If there is anything but full power factor compensation, the reactive (imaginary, jX_{WPF}) component is positive such that the current through and voltage across the impedance are out of phase and reactive power is consumed. For this option, the voltage profile at the generator terminals is required and therefore all the impedances need to be reflected to the voltage level at the generator. Fundamentally, it simulates the injection of current from the WPP in steps and calculates the voltage dropped across the Thevenin impedance at each step. This builds up number of points for the voltage at the generator terminals as the power injected increases.

Figure 10 gives simulation results. The PV curves for the above problem has been drawn for 0° , 10° leading and 20° leading power factor angle. From the curve, we obtain that value of P_L increases from lagging to leading power factor. We also obtain that there are two values of U_L for a given P_L except at P_{Lmax} . The curves are shown in Figures 10a and b. This graph shows that, following the $pf = 1$ from left to right, the voltage rises as the current injected increases and the power increases to about 21.3 MW. Then after 21.3 MW the voltage starts to drop until the critical point where the rate of decrease in voltage is

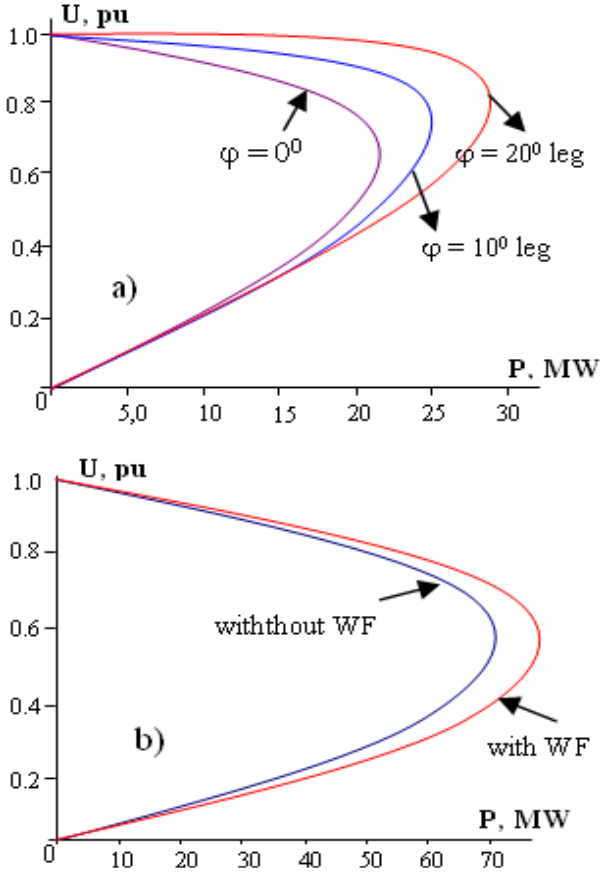


Figure 10. PV characteristics at PCC (a) and Phan Rý (b) under connected and unconnected WP condition.

faster than the rate of increase in the current injected and the power actually drops. This (the nose point) is the onset of voltage instability. From this, it can be seen that (1) approximately a maximum of 21.3 MW power can be injected without instability, and (2) reactive power control is necessary so that the WPP can be operated at, or very close to, unity power factor. If the power factor drops, it can be seen that operation is much too close to the point of voltage instability. Furthermore, the basic compensation known as “no-load” compensation is insufficient. What all this means, in practice, is that if the power factor compensation units fail then WP production must be stopped.

Line active power losses

Active power loss in the transmission line can be calculated by the Equations (7) to (8) (Kundur, 1994).

$$P_{loss_line} = 3Z_{line} |I_{grid}|^2 = 3Z_{line} \frac{|P_{grid}^2 + Q_{grid}^2|}{U_{grid}^2} \tag{7}$$

Total active power losses under full-load and no-load conditions at different wind speed (4, 8, 12, and 20 m/s) are calculated according.

$$P_{Total_loss} = P_{grid} + P_{DFIG} - P_{load} \tag{8}$$

Where $P_{Total Loss}$ is the total line power losses, P_{grid} the grid delivered power, P_{DFIG} the WP delivered power and P_{load} the power consumed by the load. According to Equation (7), any reduction in P_{grid} or Q_{grid} , reduces the power losses. This reduction of P_{grid} or Q_{grid} may be compensated by the WP.

Figure 10 gives simulation results. As the results show, with full load, the active losses reduce when the wind speed increases due to an increasing injected power from the WP. In contrast, with no-load an increasing wind speed raises the losses. The reason for this is the lengthy power transmission lines between the WP and grid [Equation (7 and 8)].

Transient stability

For transient stability evaluation, a series of simulations are performed considering different operating conditions. The following scenarios are examined: (1) Applying a short circuit fault that is cleared after 200 ms, (2) Connecting and disconnecting load, (3) WT operation under the fault condition, (4) WTs operation for the connected load condition, (5) WT operation with disconnection from the WP bus. At $t = 5$ s, a temporary three phase short circuit is placed on the load bus. After fault clearing, the load is disconnected from the load bus. The load is connected again at $t = 6.2$ s.

Simulation results are shown in Figures 11 and 12. During fault, all the DFIG turbines have zero outputs; but, after fault clearance, all of them experience short term motor behavior. This is due to energy attraction by the turbines. For brevity, only two turbine behaviors are presented in the figures. However, the system becomes stable after a short time.

WTs-DFIG operation during local load connection is also investigated and results are shown at Figure 13. This figure consists of the WP voltage, active and reactive power, the rotor speeds of the two turbines, and their pitch angle variations during this condition. The WT rotor speeds as a transient stability indicator show a stable behavior. Finally, Figure 14 shows the result when one of the DFIG is disconnected from the WT.

Conclusions

The research and simulation results have shown that the DFIG improves the voltage profile and the voltage stability of the load bus. In addition, this impact is

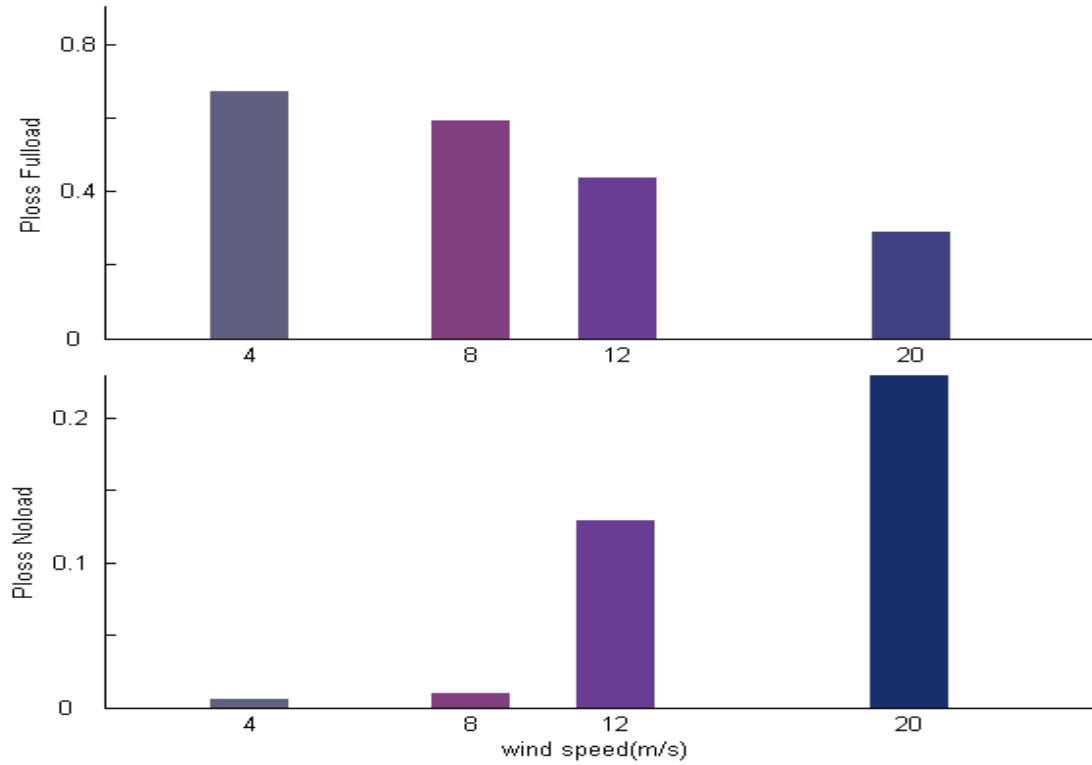


Figure 11. Active power losses at full load and no-load.

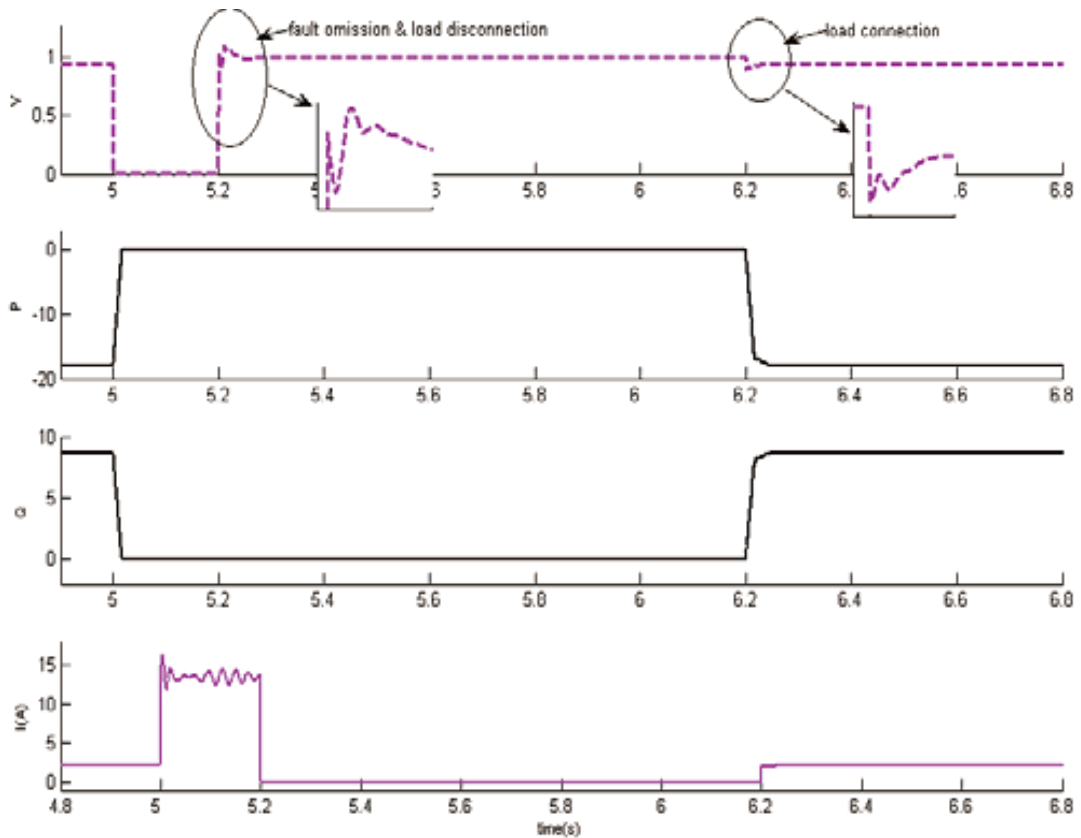


Figure 12. Three-phase fault on the load bus.

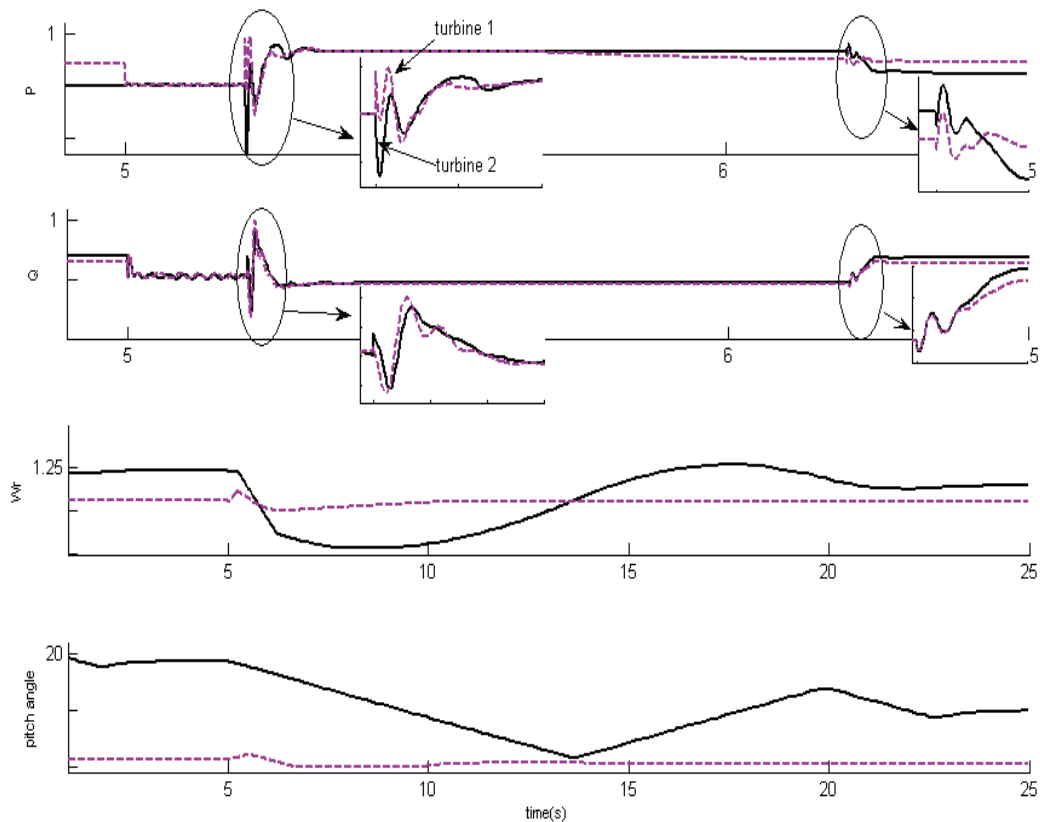


Figure 13. DFIG operation for three-phase fault condition.

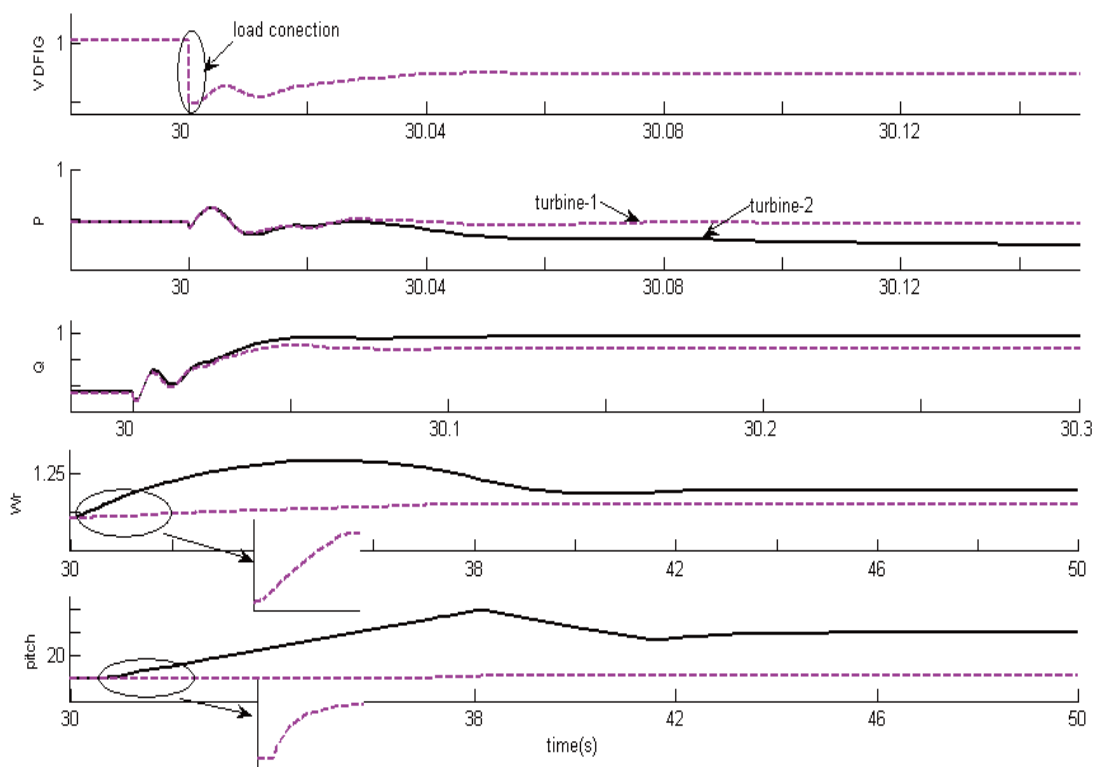


Figure 14. Turbine disconnection condition.

confirmed at low wind speed 4 m/s (low generation). During faults, all the DFIG turbines have zero outputs; but after fault clearance all of them experience short term motor behavior; however the system remains stable after that. In general, the connection of DFIG improves the stability of the system and the load voltage. Wind power generation with DFIG provides better performance for terminal voltage recovery after the load connects suddenly.

REFERENCES

- Francoise M, Bikash PC (2005). Modelling and Small-Signal Analysis of a Grid Connected Doubly-Fed Induction Generator; IEEE Trans. Power Syst. 18:803-809.
- Joris S (2005). Impact of Wind Energy in a Future Power Grid; PhD thesis, Katholieke Universiteti Leuven, Leuven.
- Johannes GS (2003). Wind Power: Modelling and Impact on Power System Dynamics; PhD thesis - Technische Universiteit Delft.
- James DB (1988). Factors influencing the protection of small-to-medium size induction generators. IEEE Trans. Ind. Appl. 24:5.
- Tony B, David S, Nick J, Ervin B (2004). Wind Energy Handbook; John Wiley & Sons Ltd, Reprinted, March.
- RISØ (2006). Feasibility Assessment and Capacity Building for Wind Energy Development in Cambodia, Philippines and Vietnam; November.
- Trinh TC (2008). Voltage stability analysis of grid connected wind generators; International Conference on Electrical Engineering; Japan.
- Sujatha K (2006). Impact of Distributed Generation on Distribution Contingency Analysis; PhD thesis, Mississippi State University, May.
- Kundur P (1994). Power System Stability and Control. Mc. Graw Hill. New York.